

Design, Development, and Evaluation of a Bionic Knee-Ankle-Foot Orthosis Retrofit for Walking Gait Normalization

Syamantak Payra and Krishnan Mahadevan

Manuscript accepted for publication in the
IEEE Transactions on Medical Robotics and Bionics (IEEE T-MRB)
a journal of the *IEEE Robotics and Automation Society*

(submitted Jan 29, 2021; revised Apr 23, 2021; accepted May 31, 2021)

DOI: *to be displayed, pending IEEE online publication*

© 2021 IEEE. *Personal use of this material is permitted. Permission from IEEE must be obtained for all other uses, in any current or future media, including reprinting/republishing this material for advertising or promotional purposes, creating new collective works, for resale or redistribution to servers or lists, or reuse of any copyrighted component of this work in other works.*

Design, Development, and Evaluation of a Bionic Knee-Ankle-Foot Orthosis Retrofit for Walking Gait Normalization

Syamantak Payra, *Student Member, IEEE*, and Krishnan Mahadevan

Abstract—A smart bionic leg orthosis (SBLO) was created by engineering an electromechanical retrofit to a conventional, fixed knee-ankle-foot orthosis (KAFO). The SBLO detects the wearer’s walking motion and intelligently bends the brace at the proper time during the walking cycle, replicating healthy knee function. Whole-body walking gait data was collected, analyzed, and statistically modeled to evaluate the SBLO and assess control algorithm robustness. Kinetic and kinematic analyses show the SBLO meets critical human leg motion parameters, indicating a partial restoration of limb functionality, and biomechanical simulations suggest the SBLO can reduce patient energy expenditure by more than 30%. Test results from a limb affected by post-polio syndrome show up to 99.84% normalization of eight walking gait characteristics across multiple mobility scenarios when using the SBLO rather than a fixed KAFO, including >75% reductions in gait pathologies. The SBLO is inexpensive yet offers more functionality than state-of-the-art solutions, by providing dynamic motion assistance to aid the wearer during walking.

Index Terms—assistive technology, biomedical engineering, legged locomotion, prosthetics, rehabilitation robotics

I. INTRODUCTION

KNEE-Ankle-Foot Orthoses (KAFOs) are orthotic devices that stabilize the knee joint and assist the leg. KAFOs, commonly known as leg braces, are required by nearly 7 million individuals in the United States alone who lack leg muscle function due to illnesses or injuries including poliomyelitis, multiple sclerosis, stroke, muscular dystrophy and spinal cord injuries [1],[2]. However, up to 80% of knee-ankle-foot orthosis wearers express dissatisfaction with their orthotics [3]. Normal walking has two phases: stance phase, when a leg bears the body weight, and swing phase, when the knee bends and the leg swings forward. Conventional KAFOs have a locking knee joint, which allows for weight to be placed on the nonfunctional leg during stance phase, and can be unlocked for sitting [4]. However, this causes walking gait pathologies such as ‘hip hike,’ in which the hip on the affected side must be employed excessively to lift the leg off the ground, and circumduction, in which the affected leg must be swung in an arc to take a step forward [5]. This abnormal walking gait leads to increased

energy expenditure, fatigue, and pain [6]. More advanced “Stance-Control” KAFOs attempt to enable a more natural knee flexion by automatically locking and unlocking the knee joint during walking [3]. Some implementations utilize mechanical pendulums or force sensors at the bottom of the orthosis to determine the proper portion of the walking cycle in which to unlock the knee joint [7]. However, such devices can only benefit the patients who have sufficient hip/foot strength to activate these mechanisms. Presently, the most advanced KAFOs utilize variable-flow hydraulic damping to change the friction of the knee joint in various phases of the walking cycle. Friction is decreased during the swing phase to allow for bending of the knee, and increased during the stance phase so the orthosis can support the weight of the wearer and resist bending [8]. However, such orthoses are expensive, require additional training and rehabilitation to use correctly, and can be contraindicated in patients without enough residual muscle function to facilitate a swing during walking [9],[10].

There is no commercially available orthotic device that actively assists the wearer to bend the knee during walking, compared to the passive support offered by conventional KAFOs [1],[11]. Hovorka, Geil, and Lusardi note that an ideal orthosis should optimize three key factors – control, comfort, and cost – while considering the wide range of neuromuscular or musculoskeletal impairments that necessitate the use of a knee-ankle-foot orthosis [12]. Projected benefits of using rehabilitative robotics to assist users in bending their leg include restoring natural walking gait and reducing excess energy expenditure during walking, which can reduce the pain and discomfort felt by wearers of knee-ankle-foot orthoses [13].

The goal of this work was to create a smart bionic leg orthosis (SBLO) retrofit that can confer biological joint and limb motion characteristics to a fixed KAFO, thereby enhancing wearer mobility. In this paper, Section II provides an overview of first- and second-generation SBLO devices. Section III and IV describe mechanical, electrical, and software aspects of device development. In Section V, device evaluation is described and results are displayed and discussed. Sections VI and VII contain applications of the SBLO, conclusions, and future work.

© 2021 IEEE. Personal use of this material is permitted. Permission from IEEE must be obtained for all other uses, in any current or future media.

Manuscript submitted 1/29/21; revised 4/23/21; accepted 5/31/21. This work was supported in part by the Clear Creek Education Foundation, a 501(c)(3) nonprofit, using educational grant funding provided by LyondellBasell.

S. Payra was with Clear Brook High School, Friendswood, TX 77546 USA. He is now with the Department of Electrical Engineering and Computer Science, Massachusetts Institute of Technology, Cambridge, MA 02139 USA.

K. Mahadevan is a Faculty with the Department of Information Technology and Center for Cyber Security, Green River College, Auburn, WA 98092 USA.

II. DEVICE OUTLINE

The following objectives were set for the first-generation (Gen-1) SBLO: a) to design an external retrofit module with a microcontroller and linear actuator to effectively rotate the knee joint, b) to develop methodologies for sensor positioning and feedback control to accurately determine the phase of the walking gait cycle, and c) to retrofit this system to a conventional KAFO. Then, a second-generation (Gen-2) retrofit was designed and developed to improve upon the capabilities of the Gen-1 SBLO. The objectives were: a) to create an affordable, smart bionic retrofit to a conventional KAFO, including i) designing a faster, more powerful linear actuator that more effectively rotates the knee joint and ii) optimizing the placement of the actuator along two axes for greatest speed and range of motion, b) to develop new algorithms for the SBLO to intelligently adapt to changes in terrain or walking speed, and c) to design a user-friendly control interface in the form of an Android application for a smartwatch/smartphone that communicates with the SBLO via Bluetooth and offers hands-free voice command recognition.

Both generations of the SBLO were designed as retrofits onto a base KAFO, made of thermoplastic and metal supports, rather than requiring the (potentially costly) fabrication of a new KAFO structure [14]. This protocol allows a patient's normal KAFO to be inexpensively converted from a fixed-knee mechanism to the smart bionic motion mechanism. To provide flexion and extension of the leg, both an actuation method and a control method were required. Gen-1 SBLO components included a microcontroller (Arduino Uno), motor controller (Roboclaw IMC418), and linear actuator (Concentric LACT4-12V). Gen-2 SBLO components included a wireless microcontroller (Atmel 32u4 with Nordic Bluetooth module, Adafruit), motor controller (CTRE Talon SRX), and improved linear actuator (iR3 DART, custom fabricated). For both generations, a lithium ion battery (14.8V / 3200mAh, 4 series cells) was used to power the SBLO, walking motion was detected using a 9-degree-of-freedom inertial measurement unit (Bosch BNO055, Adafruit), and a 3D printer (MakerBot Replicator 2) was used to fabricate mounting brackets using polylactic acid (PLA) filament. Fig. 1 shows the original thermoplastic KAFO and assembled Gen-1 and Gen-2 SBLO.

III. DEVICE DEVELOPMENT – MECHANICAL

The first stage of device development involved identifying an actuation mechanism and engineering a method to attach the actuator to the thermoplastic KAFO. Research indicated that a rotational motor mounted directly on the knee joint would have limited success due to the high torque required to bear weight and resist rotation during the stance phase of walking [15]. Magnetorheological dampers such as those in the Össur Rheo Knee prosthesis or the hydraulic damping system in the OttoBock C-Brace orthosis are expensive and only provide a variable friction damping force; they do not compensate for lack of muscle function [16]. Hydraulic or pneumatic pistons are bulky and require pumps or compressors to operate, with a risk of collapsing if power is lost. Consequently, linear actuator

technology was chosen: worm-gear and trapezoidal-lead-screw drive systems have an unpowered linear holding force that can support standing loads, and electric power for motion can be simply provided from a compact battery. This allows a stable holding force to be provided during stance phase, and powered flexion and extension of the knee joint could be achieved during swing phase of the walking cycle.

A. Actuator Design

For the Gen-1 SBLO, a commercial off-the-shelf (COTS)

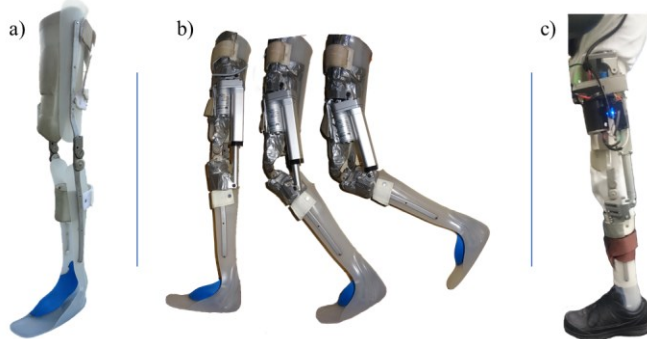


Fig. 1. Comparison of assembled braces:

- Conventional (Fixed) Knee-Ankle-Foot Orthosis,
- Gen-1 retrofit time-lapse: standing → ground push-off → fully retracted,
- Brace with Gen-2 SBLO retrofit, worn on leg with post-polio syndrome

actuator (12V input rating, 10cm (4in) stroke) was used. For the Gen-2 device, a custom actuator was designed and utilized to provide the maximum bending angle and an optimal combination of force and speed. The actuator uses an industrial DC motor (CCL PM25R), which is commonly used in robotic applications, provides high torque output, and is made with a ceramic construction which acts as thermal ballast and prevents the motor from heating up excessively – an important safety consideration for a device positioned near the body. An Acme steel lead screw (1.3cm ($\frac{1}{2}$ in) pitch, trapezoidal thread) was chosen to drive the piston of the actuator. The steel lead screw has a low friction coefficient on contact with the brass nut, which allows for efficient motion, yet the trapezoidal thread prevents the piston from moving when the motor is stopped. With this modified construction and components, the Gen-2 linear actuator had 4 \times greater force (900N vs. 220N) and 4 \times greater speed (12.7cm/s (5in/s) vs 3.18cm/s (1.25in/s)) compared to the Gen-1 actuator.

B. Gen-2 Bracket Optimization

In both the Gen-1 and Gen-2 devices, 3D-printed brackets serve to attach the retrofit mechanism to the conventional KAFO. Brackets were designed in CAD software (Autodesk Inventor) and then 3D-printed using a MakerBot Replicator 2. For the Gen-1 device, basic support brackets were created and attached to the thermoplastic KAFO using adhesives. In Gen-2, there were three additional objectives for the bracket design: 1) to design a stronger bracket that can withstand the additional force output of the Gen-2 actuator, 2) to form a sturdier connection to the thermoplastic KAFO, and 3) to optimize bracket positioning for maximum force and speed of the SBLO. To accomplish these objectives, the brackets were first contoured and designed with stress relief structures and bolt holes to

attach it to the brace. Then, objective functions were created to find the optimal upper bracket and lower bracket lengths, and position of the actuator parallel to the orthosis that would maximize the speed, foot force, and range of motion.

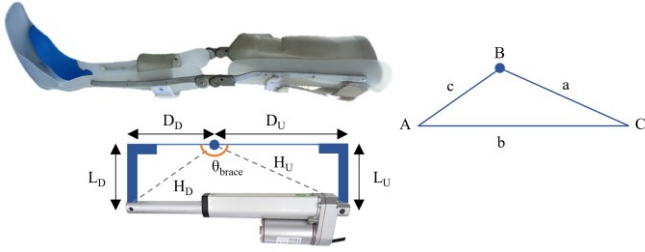


Fig. 2. Schematic of actuator and bracket positioning on brace.

L_U and L_D are the lengths of the upper and lower brackets, measured perpendicular to the orthosis. Distances D_D and D_U are the distances of each bracket from the joint. θ_{brace} is the KAFO knee angle.

The triangle (right) represents the geometry of the virtual segments used in the angular displacement calculations, where c corresponds to hypotenuse H_D , a corresponds to hypotenuse H_U , and b corresponds to actuator length.

Brace angle $B(t)$ changes as the actuator (length $b(t)$) retracts/extends. B_{max} and b_{max} are the maximum angle and actuator lengths, respectively.

Law of Cosines calculation:

$$2ac \cos(B) = a^2 + c^2 - b^2, \text{ or } B = \cos^{-1} \left(\frac{a^2 + c^2 - b^2}{2ac} \right)$$

$$\therefore a = H_U = \sqrt{D_U^2 + L_U^2} \text{ and } c = H_D = \sqrt{D_D^2 + L_D^2}$$

$$\therefore B_{max} = \cos^{-1} \left(\frac{D_U^2 + L_U^2 + D_D^2 + L_D^2 - b_{max}^2}{2\sqrt{D_U^2 + L_U^2}\sqrt{D_D^2 + L_D^2}} \right) \text{ and } B(t) = \cos^{-1} \left(\frac{D_U^2 + L_U^2 + D_D^2 + L_D^2 - b(t)^2}{2\sqrt{D_U^2 + L_U^2}\sqrt{D_D^2 + L_D^2}} \right)$$

where $b(t) = b_{max} - (\text{actuator speed} \times \text{time})$

$$\theta_{brace}(t) = 180^\circ - (B(0) - B(t))$$

$$\theta_{brace}(t) = 180^\circ - \left[\cos^{-1} \left(\frac{D_U^2 + L_U^2 + D_D^2 + L_D^2 - b_{max}^2}{2\sqrt{D_U^2 + L_U^2}\sqrt{D_D^2 + L_D^2}} \right) - \cos^{-1} \left(\frac{D_U^2 + L_U^2 + D_D^2 + L_D^2 - b(t)^2}{2\sqrt{D_U^2 + L_U^2}\sqrt{D_D^2 + L_D^2}} \right) \right] \quad (1)$$

B1) Bracket Optimization for SBLO Angle & Speed

The first part of bracket designing involved comparing how modifying bracket lengths and actuator position would impact a) how far and b) how fast the SBLO leg would bend. Fig. 2 shows the geometric layout of the bracket assembly and (1) is used to calculate the angle of the brace, $\theta_{brace}(t)$, at any given time during motion, given the parameters of bracket lengths, actuator positioning (parallel to brace), and the length of the Gen-2 actuator (depending on how far it has been retracted). $\theta_{brace}(t) = B_{max} = 180^\circ$ when the actuator is fully extended; i.e., when $b(t) = b_{max} = 35.6\text{cm}$ (14in) at $t = 0\text{s}$. Two metrics can be derived from (1): First, the smallest angle to which the actuator can be bent, B_{min} , can be calculated based on the length of the actuator when fully retracted; i.e., when $b(t) = b_{min} = 25.4\text{cm}$ (10in). This allows us to optimize bracket parameters for maximum range of motion in knee flexion. Second, the rate of bending can be found by differentiating the expression for $\theta_{brace}(t)$, when b is a function of time ($b(t) = b_{max} - (\text{actuator speed} \times \text{time})$). This allows us to optimize bracket parameters for maximum knee-bending speed.

B2) Bracket Optimization for SBLO Torque & Force

Since torque (τ) = force \times lever arm, and the force from the

actuator is acting on the lower bracket, a virtual lever arm H_D was constructed for calculation purposes (Fig. 3). Thus, the torque acting on the lower leg is given by the component of the force F_A that is perpendicular to H_D , multiplied by the distance from the brace knee joint to the point of application of the force, or $\tau = F_A \sin A \times H_D$. As a result of this torque, the foot applies a reaction force F_F to the ground, perpendicular to virtual line segment H_S , calculated using the relationship $F_F = \tau/H_S$.

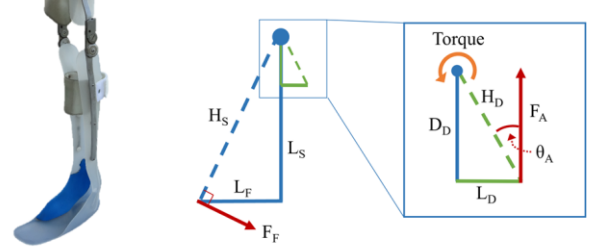


Fig. 3. Schematic of lower leg showing knee joint torque and foot force.

L_S and L_F are the lengths of the shank and foot segments, and H_S is the hypotenuse. F_A is the force exerted by the actuator on the bracket, and F_F is the force exerted by the foot upon the ground. θ_A is the angle between the actuator and the bracket, which increases as the actuator retracts (length b in Fig. 2).

Knee joint torque calculation:

$$2bc \cos(A) = b^2 + c^2 - a^2, \text{ or } A = \cos^{-1} \left(\frac{b^2 + c^2 - a^2}{2bc} \right)$$

$$\therefore A = \cos^{-1} \left(\frac{b^2 + D_D^2 + L_D^2 - D_U^2 - L_U^2}{2b\sqrt{D_D^2 + L_D^2}} \right)$$

$$\tau = F \times H_D * \sin \left[\cos^{-1} \left(\frac{b^2 + D_D^2 + L_D^2 - D_U^2 - L_U^2}{2b\sqrt{D_D^2 + L_D^2}} \right) \right] \quad (2)$$

B3) Final Gen-2 Bracket Design Parameters

Further mathematical constraints for the functions arise from physical constraints: the distance between the upper and lower bracket must be equal to the maximum length of the actuator ($D_U + D_D = b_{max}$). The lower bounds of D_U and D_D (i.e., how high the lower bracket can be or low the upper bracket can be) are constrained by the shape of the thermoplastic KAFO, since the plastic segments end some distance away from the knee joint. The length of the upper bracket (L_U) is limited by the ergonomics of the brace; if the bracket was too long, it would extend into the seat when in a sitting position. In addition, it is preferred to mount the actuator higher on the limb, as this keeps the swinging mass closer to the axis of rotation, helping decrease inertia of the limb.

Based on (1), (2), and these physical constraints, MATLAB was used to plot characteristic curves of the bracket-positioning solution space. Fig. 4 (i) demonstrates that the motion of the SBLO is faster when the upper bracket distance (from the knee joint) is either very small or very large. Fig. 4 (ii) demonstrates that the SBLO can bend back further when the brackets have shorter lengths (perpendicular to the brace). Fig. 4 (iii) demonstrates that greater foot forces are achievable when the lower bracket is closer to the knee joint and the bracket itself is longer. Both Fig. 4 (i) and (ii) were derived from the equations in Section III-B1. Fig. 4 (iii) was derived from the foot force calculations in Section III-B2.

These factors were set as constraints to solve the objective functions simultaneously with the Excel SOLVER toolkit.

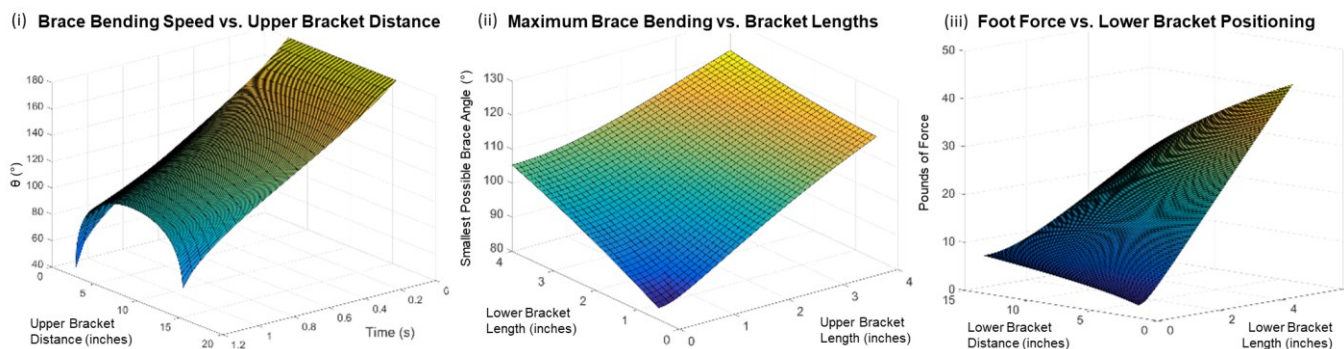


Fig. 4. Solution curves delineating SBLO motion characteristics based on variations in bracket dimensions and positioning.

Using the trend insight provided by these graphs along with the calculated solutions, optimal values for the Gen-2 actuator were found to be: upper bracket distance $D_U = 30\text{cm}$ (12in), lower bracket distance $D_L = 5\text{cm}$ (2in), upper bracket length $L_U = 2.5\text{cm}$ (1in), and lower bracket length $L_D = 5\text{cm}$ (2in). Notably, this mathematically optimized actuator positioning corresponds closely with biological musculature, such as the location of the biceps femoris (hamstring), which aids in knee flexion [17].

IV. DEVICE DEVELOPMENT – ELECTRONICS AND SOFTWARE

The second part of device hardware development was the control electronics, which facilitate the autonomous function of the SBLO. In addition to utilizing a 30% more powerful motor controller than the Gen-1 device, the Gen-2 SBLO eliminated the need for an external processor / motor controller enclosure by mounting both components directly to the aluminum actuator body, which serves as a heatsink. Three layers of fail-safes (software limits, limit switches, and hard end stops) were also introduced as actuator safety features.

A. Gait Detection Electronics

In order to form a motion control algorithm, it was necessary to have some form of sensor feedback [18]. Foot force sensors can be unreliable on patients without foot function [12], and accelerometer data requires significant smoothing and can be easily destabilized [19]. Instead, orientation angle output (pre-processed by the Bosch BNO055 chipset) was selected for gyroscopic knee angle detection based on walking gait motion. Also, previous computerized prosthetics/orthotics have utilized sensors directly on the device, which detects the motion of the affected limb. Instead, our SBLO detects motion from the opposing limb, which enables more robust control based on explicit actions taken with the other side of the body. In the Gen-2 retrofit, a potentiometer-based leg-angle monitoring feedback loop was also incorporated to facilitate fine-tuned motion profiles for different mobility cases, such as sitting down or climbing stairs.

B. Motion Control Software

The software aspect of this work had two main components: a) an embedded algorithm for orthosis functionality, and b) a user control interface (in Gen-2).

Programming the Gen-1 SBLO retrofit involved determining the appropriate time in the walking cycle to bend the brace knee joint and carrying out a simple, identical motion for each

footstep. In the Gen-1 algorithm, the microcontroller detects the beginning and end of a step by the opposing leg, and instructs the motor controller to retract and extend the actuator, thereby initiating a footstep with the SBLO. In the Gen-2 SBLO retrofit, the walking algorithm was further improved by incorporating additional capabilities, including a) adaptive gait detection, b) automatic speed adjustment, and c) the ability to walk over uneven terrain. Additional algorithms were also created to offer functionality in multiple mobility scenarios beyond level-ground walking: going up/down ramps, going up/down stairs, entering/exiting a vehicle, and sitting/standing [20]. In total, 8 new mobility modes were created and implemented in 22 code segments to offer more versatility and intuitive user flexibility in pursuit of a bionic retrofit that can offer rehabilitative assistance throughout daily usage.

Rather than detecting each footstep at a set angle threshold as in the Gen-1 algorithms, the Gen-2 walking algorithm detection thresholds change in real-time based on the magnitude of the step detected. The algorithm measures the elapsed time between the beginning and end of a footstep with the reference (opposing) leg, monitoring the speed of walking and changing the speed of the SBLO accordingly. To allow for walking on ramps and uneven terrain, the algorithm detects the maximum knee lift angle reached as a step is begun and uses that value to account for the angle of the ground when retracting the actuator on the SBLO (more flexion if walking up a slope, less flexion if walking down a slope) [21]. Walking on stairs was implemented by programming the SBLO to clear the edge of a step, whether stepping up or down. For climbing stairs, the algorithm is designed to retract the SBLO while stepping up with the brace leg, to assist users in clearing the step. When stepping down, the actuator retracts slightly. This pushes the SBLO forward, which reduces the effort required to lift the leg before lowering it onto the next step.

Failsafe measures were also incorporated into the Gen-2 SBLO algorithm. For example, turning or taking a step backwards will not trigger a step, preventing undesired operation at incorrect times and increasing the safety of walking. In the event that a fall is detected, the brace reverts to a default extended state, allowing the wearer to use the brace as a support when returning to an upright position.

Finally, an intuitive, multi-platform user control interface was created with smartphone and smartwatch compatibility, Bluetooth capability for wireless orthosis control, and hands-free voice command recognition for ease of use. An Android

app was programmed in Java using Android Studio to use encrypted Bluetooth-based communication to send commands to the microcontroller module on the SBLO. A graphical interface allows the user to choose modes and modify settings, and voice recognition can be used hands-free to assert motion commands, offering both ease of use as well as increased safety.

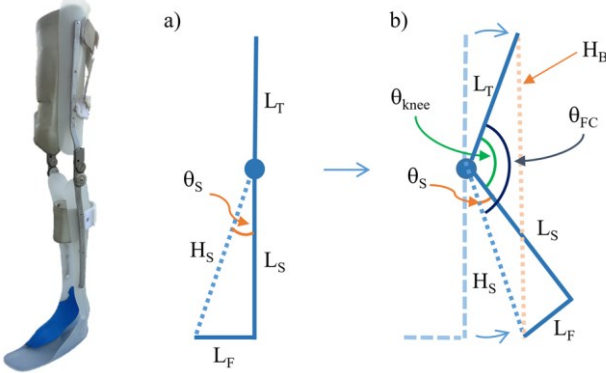


Fig. 5. Schematic of ground clearance while stepping.

L_T , L_S , and L_F represent the length of the thigh, shank, and foot segments of the brace. θ_s is the shank angle formed between the shank and virtual segment H_S . H_B corresponds to the effective brace height that must be reached in order to successfully ‘clear’ the ground for an unimpeded leg swing. To calculate the necessary knee angle θ_{knee} , a critical foot clearance angle θ_{FC} must be found that fulfills the constraint $H_B = L_T + L_S$.

Ground clearance calculation:

$$H_B^2 = H_S^2 + L_T^2 - 2 \times H_S \times L_T \times \cos \theta_{FC}$$

$$\theta_{FC} = \cos^{-1} \left(\frac{H_S^2 + L_T^2 - H_B^2}{2 \times H_S \times L_T} \right) = \cos^{-1} \left(\frac{22 + 15^2 - 34.5^2}{2 \times 22 \times 15} \right) = 136^\circ$$

$$L_T = 25\text{cm} (10\text{in}) \text{ and } L_S = 51\text{cm} (20\text{in}), \text{ so } \theta_s = \tan^{-1} \left(\frac{10}{20} \right) = 26.6^\circ$$

$$\therefore \theta_{knee} = \theta_{FC} - \theta_s = 136^\circ - 26.6^\circ = 109.4^\circ \quad (3)$$

C. Algorithm Calibration for Toe Clearance while Stepping

The distance from any hip joint to the tip of the foot is larger than the distance from the hip joint to the heel, just as how the hypotenuse of a right triangle is longer than the height. This is why wearing a locked knee joint causes ‘hip hike’: patients must lift the entire leg with their hip to avoid the toe dragging on the ground. Bending the knee solves this problem by shortening the distance from the hip joint to the toes. Once a certain angle of knee bending is reached, the toe will no longer touch the ground as the leg swings forward. The calculation in Fig. 5 uses the law of cosines to find the foot clearance angle (θ_{knee}) up to which the SBLO needs to be bent in order to clear the ground. The result from (3) allows for the SBLO motion control algorithm to be properly calibrated. Since $\theta_{brace_{max}} - \theta_{knee} = 180^\circ - 109.4^\circ = 70.6^\circ$, the SBLO must retract by at least 70.6° for full ground clearance during each step.

D. Sensor Positioning for Whole-Body Gait Data Collection

To evaluate the performance of the SBLO, walking gait data was collected from one of the authors, who is a daily wearer of a fixed KAFO due to post-polio syndrome. A whole-body gait data collection harness was constructed using 8 inertial measurement units positioned across the body as shown in Fig. 6. Data collection algorithms were implemented in MATLAB; a centralized computer establishes communications with eight

Sensor Placement	
Upper Back	UB
Lower Back	LB
Left Hip	LH
Right Hip	RH
Left Thigh	LT
Right Thigh	RT
Left Shank	LS
Right Shank	RS

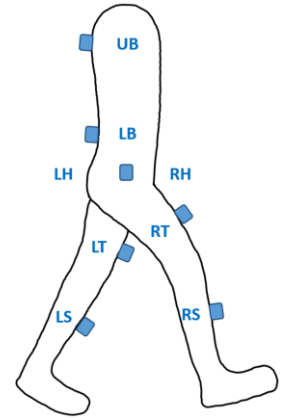


Fig. 6. Motion sensor positioning for whole-body gait data collection.

microcontrollers, which stream serial motion data from their respective sensors. Data acquisition and recording continues for the duration of walking, until a testing cycle is completed. A total of 14 motion parameters were recorded from each sensor: absolute orientation angle (relative to gravity) in X, Y, and Z axes; acceleration in X, Y, and Z axes, angular velocity around X, Y, and Z axes, quaternion-formatted (W, X, Y, Z) angular displacement, and time elapsed. Walking gait was recorded wearing the fixed brace (KAFO) and the Gen-2 retrofitted SBLO in three different mobility scenarios: level-ground walking, walking on a ramp, and walking on stairs. Four trials were conducted for each brace in each scenario, resulting in the collection of 24 total gait datasets.

TABLE I
KINETIC & KINEMATIC GAIT PARAMETER COMPARISON:

Gait Parameter	Smart Bionic Leg Orthosis		Healthy Leg
	Gen-1	Gen-2	
Actuator speed (m/s)	0.04	0.14	N/A
Actuator force (N)	220	900	N/A
Max range of motion ($^\circ$)	59.06	90.23	130.00 [23]
Initial foot force (N)	18.82	76.29	187.50 [24]
Initial torque (Nm)	10.52	42.64	46.13 [24]
Moment (Nm / kg)	0.14	0.57	0.62 [24]
Max bending speed ($^\circ$ /s)	29.65	112.38	102.94 [25]
Time to clear ground (s)	0.80	0.63	0.68 [25]
Flexion for footstep ($^\circ$)	23.70	70.80	70.00 [26]
Weight (kg)	1.13 + leg*	2.72 + leg*	9.60 [22]

Measured/calculated operational parameters for Gen-1 and Gen-2 SBLO compared to healthy leg parameters from reference literature.

*Weight of disabled leg.

V. RESULTS AND DISCUSSIONS

The study of human gait can be classified into kinematics and kinetics [22]. Kinematics is the study of the motion of bodies as linear or angular displacement and velocity over time. Kinetics is the study of the forces associated with the motion. To compare the Gen-1 and Gen-2 SBLO retrofits with literature data from healthy legs, a series of kinetic and kinematic parameters were calculated and analyzed (Table I). Kinematic parameters during average walking such as angular velocity (bending speed) and foot force, and functional limits of the mechanisms, such as maximum speed, force, torque, and foot force, were first calculated mathematically based on hardware specifications and actuator positioning parameters, then verified with the prototype [19].

Fig. 7 compares the knee joint flexion and extension for Gen-1, Gen-2, and healthy human knee motion during walking. The Gen-1 device had a low speed and range of motion (Table I), which was improved in the Gen-2 device (maximum rotational velocity increased nearly 4 \times , from 29.65 $^{\circ}$ /s to 112.38 $^{\circ}$ /s, and range of motion increased \sim 1.5 \times , from 59.06 $^{\circ}$ to 90.23 $^{\circ}$). The Gen-2 SBLO knee joint motion (Fig. 7 (a)) closely matches that of a healthy leg [27]. This is a significant improvement from both the Gen-1 SBLO, and from a fixed KAFO, which has no motion at all. The first peak in the knee flexion graphs of the Gen-2 SBLO (Fig. 7 (a)) and healthy leg (Fig. 7 (b)) indicate a slight bending of the knee to allow for shock absorption at heel-strike of the stance phase; the second peak is from the main flexion of the knee during swing phase [28]. This additional motion component was added to the Gen-2 walking algorithm to facilitate shock absorption, which was not present in Gen-1.

As a result of the increased actuator force/speed and optimized bracket positioning, the Gen-2 SBLO is able to overcome two key limitations of the Gen-1 SBLO: speed and knee range of motion. In the Gen-1 SBLO, not only was the retraction too slow for normal-speed walking, the maximum retraction was not enough to clear the ground (23.70 $^{\circ}$ in 0.80s, max bending 59.06 $^{\circ}$). With the Gen-2 device, ground clearance is possible in the time required for a normal step [24], and the range of motion is larger (70.80 $^{\circ}$ footstep in 0.63s, max 90.23 $^{\circ}$).

To quantify the physical aid offered by the retrofitted SBLO, (2) and the force-torque relationship from Section III-B1 were used to calculate the foot force transmitted to the ground. The force provided by a healthy adult's foot when taking a step is approximately 25% of body weight [16]. The linear actuator applies \sim 890N of force to the lower bracket, which results in the Gen-2 SBLO sending 76.29N of force to the ground when the orthosis retracts to take a step (2). Thus, the Gen-2 SBLO can provide 41.67% of the force of a healthy foot (75kg person). This is a considerable contribution because in a patient wearing a KAFO, this force would usually be provided by the hip, back, and shoulders [11]. By providing this foot force, the bionic orthosis alleviates the effort required from the rest of the body.

A. Predicted Energy Consumption

Doke, Donelan, and Kuo estimate that swinging the legs alone requires 1/3 of the energy cost of walking [29]. For a patient who uses a KAFO, however, excess energy expenditure is required not only to swing the leg but also to move one side of the body forward using compensatory strategies such as 'hip

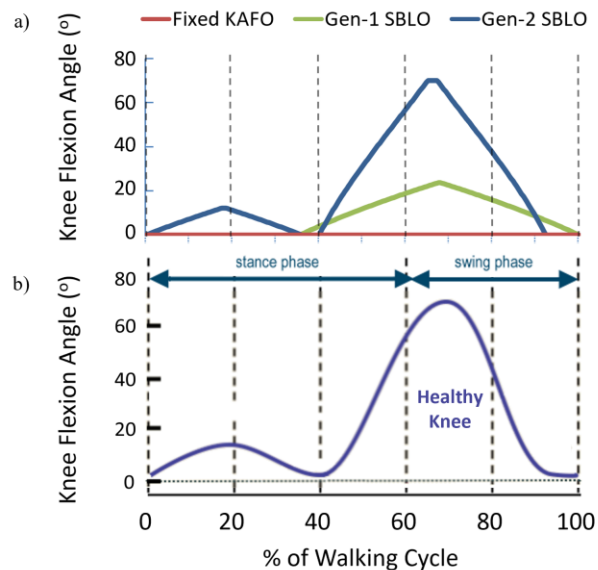


Fig. 7. Knee flexion over time with different KAFOs vs. healthy knee [28].

hike' and circumduction [12]. Biomechanical simulations were conducted in OpenSim [30] to predict the impact on the energy cost of walking with the SBLO rather than a fixed KAFO (Fig. 8). The base musculoskeletal model (normalized 75kg male) had 10 degrees of freedom and 18 muscles [31]. One modified version of this model incorporated the physical characteristics (such as segment weight, 'muscle' positioning, and force) of the Gen-2 bionic brace mechanism. A second modified model was created to reflect the restrictive properties of a fixed KAFO. Walking was simulated with these models and the energy consumption by the muscles in the lower body was calculated by OpenSim based on the methodology detailed by Umberger et al. [32]. Simulation results (Fig. 8) indicate that there may be up to a 31.33% decrease in the energy expenditure during walking when using the Gen-2 SBLO rather than a conventional, fixed KAFO.

B. Knee Joint Torque Assessment

To understand the extent to which knee joint torque was normalized with the SBLO retrofit, a Process Capability Analysis was conducted using Minitab 18. The first set of the distribution curves for torque in Fig. 9 (i) and (ii) indicate a wider distribution with low confidence. In Fig. 9 (iii), however, there is a "tighter" distribution with the bars closer together, indicating a large degree of similarity between the two datasets. The performance analysis statistics show that there is a very

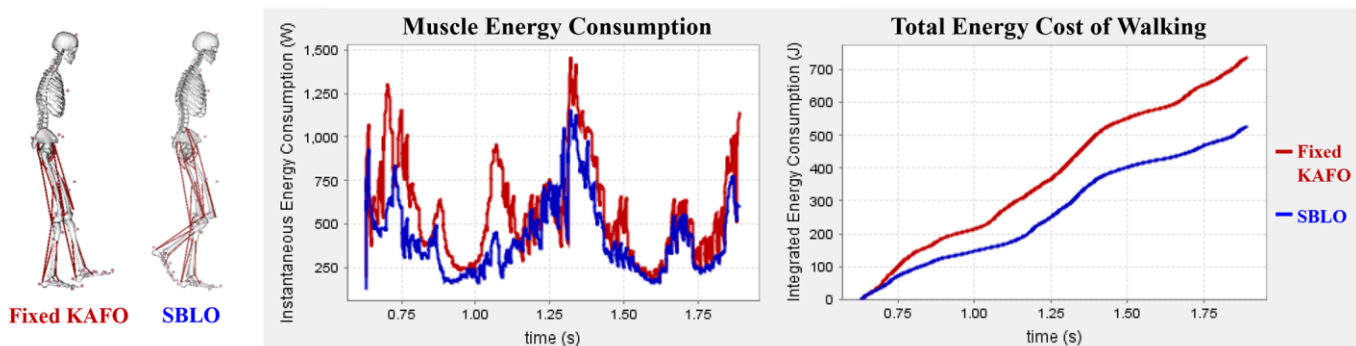


Fig. 8. Simulation of body energy consumption during walking with a conventional (fixed) KAFO, compared to the Gen-2 SBLO.

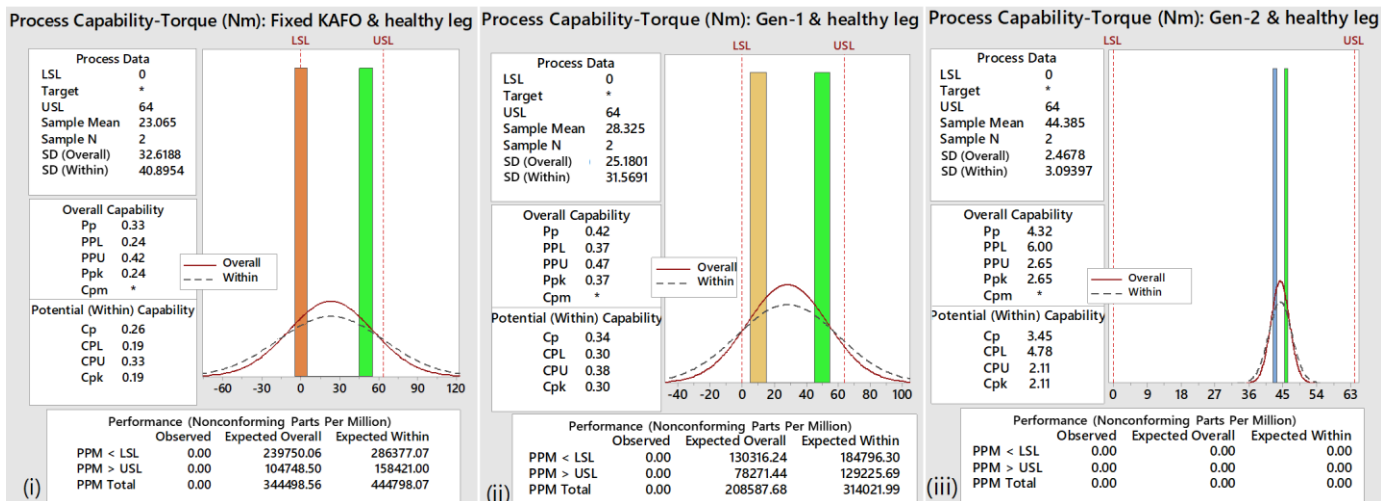


Fig. 9. Process Capability Analysis and Process Performance Analysis for knee joint torque across different test conditions.

Sample Mean = average of the two datasets, N = number of datasets, SD = standard deviation, USL = Upper Specification Limit, LSL = Lower Specification Limit. "Overall" represents predicted process capability as a normal distribution; "Within" represents observed variance in existing process data.

In the analysis of Overall Capability (Pp/Ppk), Pp indicates capability based on overall variation (lower variation = higher capability), and Ppk is a performance index normalized for long-term variation. In the analysis of Potential Capability (Cp/Cpk), Cp indicates capability based on variation within datasets, and Cpk is a performance index normalized to the specification limits. In other words, Cpk is a measure of how many times the distribution of a process can widen before it exceeds the specification limits. For a statistically well-performing process, Cp should be greater than 2.0 and Cpk should be greater than 1.5 [33].

In the performance analysis, PPM>USL and PPM<LSL refer to the number of projected nonconforming parts per million that fall above and below the Upper/Lower Specification Limits. The Upper Specification Limit (USL) is 64Nm, the maximum torque possible from the Gen-2 SBLO (Table I). The Lower Specification Limit (LSL) is 0Nm, the torque produced by the fixed KAFO. A lower value for the nonconforming part count indicates better process performance.

large difference between the conventional fixed KAFO and a healthy leg, and there is a high nonconforming part count (>440,000 PPM) (Fig. 9 (i)). This is reduced to 0 PPM nonconforming between the Gen-2 and healthy leg, indicating that the Gen-2 SBLO has very high performance within the specification limits of healthy walking. From the data in Fig. 9 (i), predicted walking with the fixed KAFO and healthy leg is reflected as a statistically poor-performing process. There is a high standard deviation and standard error of the mean (SEM) (SD overall = 32.62, SEM = 23.10), low process performance (Pp = 0.33, Ppk = 0.24), low process capability (Cp = 0.26, Cpk = 0.19), and a large confidence interval (CI) (95% CI Range = -270.0Nm to 316.1Nm). Ideally, the SD and SEM should be as low as possible, indicating consistency and low variation, the process performance and capability should be as high as possible, indicating a statistically well-performing process, and the 95% CI (the range within which 95% of the values in a particular distribution fall) should be as small as possible, indicating that the two datasets being compared are very similar. If achieved, these parameters would suggest that the two legs being compared (one of which is healthy and one of which has a KAFO or SBLO) exhibit an even and smooth walking gait. When the Gen-2 SBLO and the healthy leg are analyzed together (Fig. 9 (iii)), there is a smaller standard deviation and standard error of the mean (SD = 2.47, SEM = 1.74), better process performance (Pp = 4.32, Ppk = 2.65), better process capability (Cp = 3.45, Cpk = 2.11), and smaller confidence interval (95% CI range = 22.21Nm to 66.56Nm). There is a significant improvement in all parameters, including a 1000% smaller CI, indicating that the knee joint torque similarity between the Gen-2 SBLO and healthy leg is far greater than the similarity between the fixed KAFO and healthy leg. This demonstrates that in predictive statistical analysis

based on the torque produced at the knee joint, walking with the Gen-2 SBLO and healthy leg creates a much smoother walking gait compared to walking with a fixed KAFO and healthy leg.

C. Device Evaluation

To evaluate the functionality of the SBLO, the retrofit was tested on a limb requiring the use of a KAFO to determine whether a) the resultant walking gait would more closely resemble that of the normal leg, and b) the overall walking gait would exhibit reduced pathologies compared to walking gait while using the fixed KAFO.

C1) Walking Gait: Leg Motion in Segments & Joints

The whole-body walking gait from Fig. 6 and Section IV-D was synthesized, following methodology from [25], into four motion parameters representing leg segments and joints: shank motion, thigh motion, knee joint angle, and hip joint angle.

Fig. 10 shows comparisons of walking gait between the Fixed KAFO and the SBLO. In each graph, the left leg (whether Fixed KAFO or SBLO) is shown in blue, while the right leg (healthy leg) is shown in red. It was observed that in each case, the motion with the SBLO is much smoother and more closely resembles the motion of the healthy right leg. Importantly, there was a significant improvement in knee joint motion from the fixed KAFO to the SBLO (Fig. 10 (v-vi)). In addition, the SBLO enabled a faster self-selected walking cadence than with the Fixed KAFO (four vs. three steps in a ~7.3s time interval).

C2) Statistical Analysis of Gait Normalization

To compare walking gait between datasets, the range of motion was analyzed. The range of motion is defined as the angle difference between the extent of a step forward by that leg and the farthest back one leg goes during a step by the opposing leg. Ideally, the range of motion between the left and right leg should be as close together as possible; this would

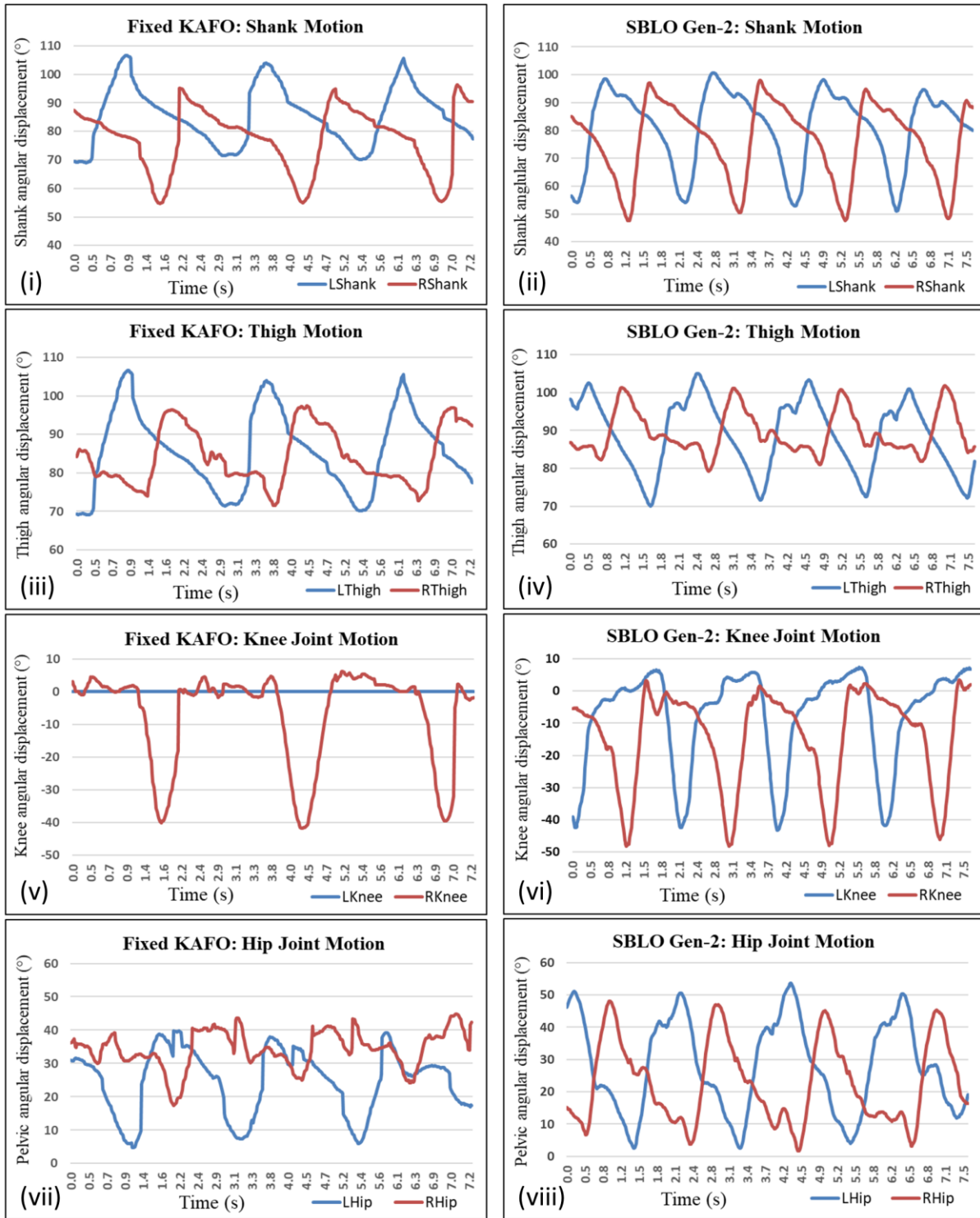


Fig. 10. Walking gait plots showing leg motion in segments and joints when wearing a fixed KAFO (i, iii, v, vii) or SBLO (ii, iv, vi, viii).

The footsteps in the graphs represent an arbitrary sample window (~ 7.3 s) from the larger gait datasets collected.

indicate that the two sides have similar walking gait.

Table II shows a statistical analysis of joint and segment motion data. For each test case, the range of motion is compared between the left leg (KAFO) and right leg (healthy) to assess whether there is a statistically significant difference in motion, which would indicate an uneven walking gait. In a normal (healthy) walking gait, there should not be a statistically significant difference between the range of motion of the left and right legs. For both leg segments, shank & thigh (FB-

LShank vs RShank, FB-LThigh vs RThigh) and both leg joints, knee & hip (FB-LKnee vs RKnee, FB-LHip vs RHip), there is a statistically significant difference ($p < 0.05$) between the range of motion of the fixed brace on the left leg and the healthy right leg. This indicates that walking gait with the fixed KAFO is uneven, as significant disparities exist between the motion of the left (KAFO) and right (healthy) legs. However, for both leg segments (SBLO-LShank vs RShank, SBLO-LThigh vs RThigh) and both leg joints (SBLO-LKnee vs RKnee, SBLO-

TABLE II
T-TEST ANALYSIS: FIXED KAFO VS GEN-2 SBLO

Sensor Position / Segment	Range of motion angle (°)				T-test P	Statistically Significant Difference (P < 0.05)	Indication
	Mean	SD	N	SEM			
FB-LShank	34.19	2.28	17	0.55	0.0001	Yes	Fixed Brace Gait Abnormal
RShank	40.08	2.43	17	0.59			
FB-LThigh	34.19	2.28	17	0.55	0.0001	Yes	
RThigh	24.38	2.84	17	0.69			
FB-LKnee	0.00	0.00	17	0.00	0.0001	Yes	
RKnee	43.42	1.78	17	0.43			
FB-LHip	33.51	2.97	8	1.05	0.0001	Yes	
RHip	19.19	2.62	8	0.93			
SBLO-LShank	44.66	2.21	16	0.55	0.0616	No	Bionic Brace Gait Normalized
RShank	46.38	2.77	16	0.69			
SBLO-LThigh	32.30	3.10	16	0.78	0.6320	No	
RThigh	32.97	1.91	6	0.85			
SBLO-LKnee	49.33	1.86	16	0.47	0.9192	No	
RKnee	49.26	2.01	16	0.50			
SBLO-LHip	45.79	5.19	8	1.72	0.1152	No	
RHip	42.63	2.10	8	0.74			

FB = Fixed Brace (KAFO). SBLO = Smart Bionic Leg Orthosis (Gen-2).

LHip vs RHip), there is not a statistically significant difference ($p > 0.05$) between the range of motion of the SBLO on the left leg and the healthy right leg. This indicates that the SBLO is able to normalize walking gait of the disabled leg, and there is no longer a statistically significant difference between the motion of the healthy leg and the brace leg.

C3) Process Capability Analysis: Gait Improvement

To understand the extent to which walking gait was normalized, a process capability analysis was conducted in Minitab 18. The first part of the process capability analysis,

composed of the graphs in Fig. 11, illustrates the discrepancies between the ranges of motion of the datasets in each comparison. The x-axis shows angle (range of motion, °), and each vertical bar represents one dataset. The first set of graphs (Fig. 11 (i-iv)) compares the motion of the fixed KAFO and the healthy right leg. The large horizontal distance between the two bars reflects the large motion discrepancy, and the distribution curves are wider, indicating greater variability in the walking gait when walking with the fixed KAFO. In the second set of graphs (Fig. 11 (v-viii)), there is a “tighter” distribution with the bars closer together. This indicates that there is lower variability in the walking gait when walking with the SBLO, and that the motion of the SBLO and the healthy right leg are very similar.

C4) SBLO Performance: Nonconforming Part Analysis

The second part of the process capability analysis is the nonconforming part analysis, listed in Table III, which measures the number of nonconforming parts per million in the process. A lower value for the nonconforming part count (in parts per million, or PPM) indicates better process performance. For all the motion analyses with the fixed KAFO, there are very high nonconforming part counts. For example, the highest value is 500,000 PPM (FB-LKnee vs RKnee), which indicates that the knee motion within that pairing falls outside of the bounds (PPM < LSL) of normal (“healthy”) walking data half of the time – corroborated by the fact that the fixed KAFO knee joint, which comprises half the dataset, does not have any knee motion. However, for the motion analyses with the SBLO, the nonconforming part counts are all reduced to near zero. This indicates that the motion consistently falls within the bounds of healthy walking, reinforcing the previous analyses that show

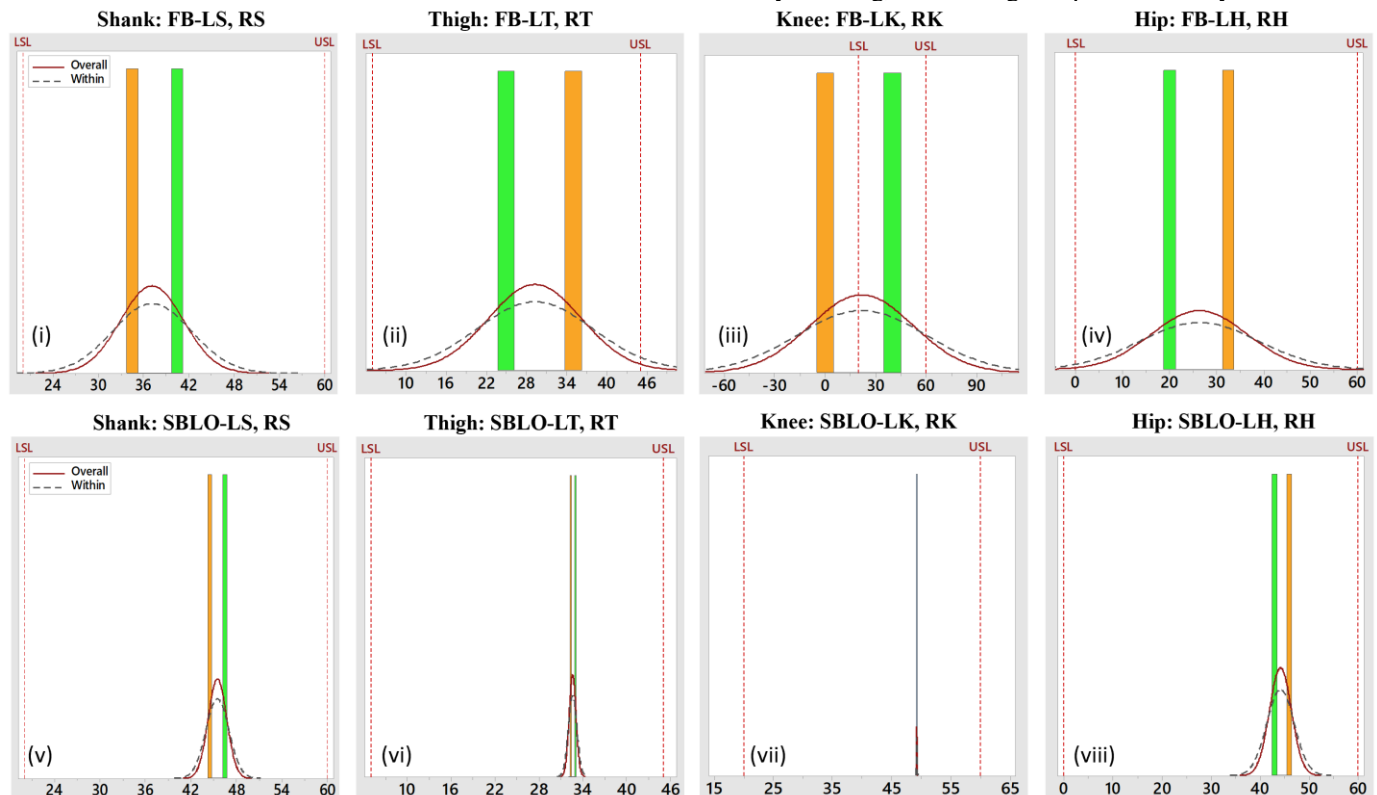


Fig. 11. Process capability analysis: (i-iv) shows segment and joint motion when walking with Fixed KAFO (“FB”, orange) and healthy right leg (green). (v-viii) shows segment and joint motion walking with Gen-2 SBLO (“SBLO”, orange) and healthy right leg (green). For terminology, see Fig. 9 caption.

TABLE III
PROCESS CAPABILITY ANALYSIS: PERFORMANCE (NONCONFORMING PARTS PER MILLION) IN WALKING GAIT

Fixed KAFO	FB-LShank, RShank			FB-LThigh, RThigh			FB-LKnee, RKnee			FB-LHip, RHip		
	Observed	Expected Overall	Expected Within	Observed	Expected Overall	Expected Within	Observed	Expected Overall	Expected Within	Observed	Expected Overall	Expected Within
PPM<LSL	0.00	19.43	516.21	0.00	231.81	2615.90	500000.00	477792.13	482283.31	0.00	4630.43	18964.81
PPM>USL	0.00	0.02	5.96	0.00	11741.60	35382.33	0.00	106175.54	159934.12	0.00	444.95	4016.94
PPM Total	0.00	19.45	522.17	0.00	11973.41	37998.23	0.00	583967.67	642217.43	0.00	5075.37	22981.75

SBLO Gen-2	SBLO-LShank, RShank			SBLO-LThigh, RThigh			SBLO-LKnee, RKnee			SBLO-LHip, RHip		
	Observed	Expected Overall	Expected Within	Observed	Expected Overall	Expected Within	Observed	Expected Overall	Expected Within	Observed	Expected Overall	Expected Within
PPM<LSL	0.00	0.00	0.00	0.00	0.00	0.00	0.00	0.00	0.00	0.00	0.00	0.00
PPM>USL	0.00	0.00	0.00	0.00	0.00	0.00	0.00	0.00	0.00	0.00	0.00	0.01
PPM Total	0.00	0.00	0.00	0.00	0.00	0.00	0.00	0.00	0.00	0.00	0.00	0.01

For Process Capability Analysis terminology, see Fig. 9 caption.

that the SBLO retrofit normalizes walking gait.

The third part of the process capability analysis, presented in Table IV, is a process performance analysis that includes a set of metrics for a comprehensive measure of the individual and relative statistical performance. The top half of the table contains the reference analysis for leg segment and joint motion when walking with the fixed KAFO; the lower half contains the analysis for leg segment and joint motion when walking with the SBLO. The improvement in each walking gait parameter is noted in the final column. We observe that the SBLO is able to normalize shank motion by 70.79%, thigh motion by 93.25%, knee joint motion by 99.84%, and hip joint motion by 78.08%.

D. SBLO Performance Summary

Table V quantifies the benefit of the Smart Bionic Leg Orthosis (SBLO) by listing the observed improvement compared to a Fixed KAFO in eight key kinetic/kinematic motion parameters when tested on a leg with post-polio syndrome, plus one simulated parameter (energy consumption). The SBLO normalized shank motion, thigh motion, hip motion, and knee motion; in addition, the SBLO was also able to reduce gait pathologies: upper body tilt was reduced by 41.47%, and circumduction was reduced by 78.08%. These factors were able to increase wearer mobility, such as the 90% increase in maximum walking speed observed. The unique functionality of

the SBLO is due to its dynamic, powered assistance for knee joint bending, as compared to leading commercially available KAFOs, which simply lock/unlock or dampen the motion of the knee joint [3],[7],[9]. Not only does the SBLO retrofit provide intelligent assistance that recognizes and adapts to variations in terrain, gait, speed, and mobility scenarios, it also maintains a minimal cost point (\$600 retrofit onto a conventional KAFO, vs. up to ~\$92,000 retail price for a new standalone brace [10]).

TABLE V
PERFORMANCE IMPROVEMENT: GEN-2 SBLO VS FIXED KAFO

Parameter	Observed Improvement
Knee joint motion	Normalized by 99.84%
Upper leg motion	Normalized by 93.25%
Hip joint motion	Normalized by 77.93%
Lower leg motion	Normalized by 70.79%
Energy consumption	Reduced by 31.33%
Leg circumduction	Reduced by 78.08%
Upper body tilt	Reduced by 41.47%
Foot force	Up to 200.00% greater
Walking speed	Up to 90.00% greater

VI. APPLICATIONS

Unlike other leg orthoses, the retrofitted SBLO actively aids wearers of a KAFO during walking by utilizing a linear actuator to provide knee flexion for ground clearance during swing

TABLE IV
PROCESS CAPABILITY ANALYSIS: IMPROVEMENT IN WALKING GAIT PERFORMANCE, FIXED KAFO VS SBLO

Sensor Position	General					Overall Capability				Potential Capability (within)				Process Performance	
	LSL	USL	Mean	SD (overall)	SD (within)	Pp	PpL	PpU	Ppk	Cp	CpL	CpU	Cpk	95% CI	Improvement
FB-LShank, RShank	20	60	37.14	4.16	5.22	1.60	1.37	1.83	1.37	1.28	1.09	1.46	1.09	-0.28, 74.55	---
FB-LThigh, RThigh	5	45	29.28	6.94	8.69	0.96	1.17	0.76	0.76	0.77	0.93	0.60	0.60	-33.04, 91.61	
FB-LKnee, RKnee	20	60	21.71	30.70	38.49	0.22	0.02	0.42	0.02	0.17	0.01	0.33	0.01	-254.11, 297.63	
FB-LHip, RHip	0	60	26.35	10.13	12.69	0.99	0.87	1.11	0.87	0.79	0.69	0.88	0.69	-64.63, 117.33	
SBLO-LShank, RShank	20	60	45.52	1.22	1.52	5.48	6.99	3.97	3.97	4.37	5.58	3.17	3.17	34.59, 56.45	70.79%
SBLO-LThigh, RThigh	5	45	32.64	0.47	0.59	14.07	19.44	8.70	8.70	11.22	15.51	6.94	6.94	28.38, 36.89	93.25%
SBLO-LKnee, RKnee	20	60	49.29	0.05	0.06	134.69	197.28	72.09	72.09	107.43	157.36	57.50	57.50	48.85, 49.74	99.84%
SBLO-LHip, RHip	0	60	44.21	2.23	2.80	4.48	6.60	2.36	2.36	3.57	5.26	1.88	1.88	24.13, 64.29	77.93%

For Process Capability Analysis terminology, see Fig. 9 caption.

phase. In contrast to KAFOs available on the market that are not suited for patients with minimal muscle function, this powered bionic retrofit can even aid patients with little to no quadriceps strength. The bionic leg orthosis is ‘smart’ not only due to its ability to interface with smartwatches / smartphones, but also because of the intelligent algorithms that offer multiple modes of functionality and allow the SBLO to adapt to changes in terrain, walking speed, and walking pattern.

By decreasing gait pathologies that destabilize the upper body, the SBLO can offer a safer walking experience. As part of the compensatory strategies exhibited by a patient walking with a conventional KAFO, the upper body must move oblique to the path of motion, to aid swing of the nonfunctional leg forward. However, this leads to instability even when coupled with a walking aid such as a cane, due to the shift in the center of gravity and the abnormal gait, and often results in slips, falls, or stumbles [2]. With the SBLO retrofit, walking motion for each leg can occur in two parallel planes, relieving the need to compensate with the upper body for a lack of function of the lower limbs thereby decreasing the risk of falls. In addition, failsafe measures have been incorporated into the brace operation algorithm. For example, because the microcontroller detects a step forward by the right leg, turning or taking a step backwards will not trigger a step by the Smart Bionic Brace on the left leg, preventing undesired operation at incorrect times.

The SBLO also has further applications beyond the demand and great need for a better KAFO, such as usage as a therapeutic device. Rather than manual muscle resistance training or large hospital rehabilitation devices, this retrofitted leg orthosis is an inexpensive, self-contained robotic rehabilitation solution with adjustable speed, motion, and tension for knee flexion and extension, offering a more flexible and versatile alternative than existing methods and equipment. To implement such a device on a larger scale, by retrofitting many patients’ KAFOs, the algorithm must be flexible to accommodate individual gait patterns. This has been accounted for in the SBLO, and only one parameter needs to be changed based on a preliminary gait analysis to personalize the algorithm to a patient’s walking gait: the baseline threshold to detect a step, which depends on the patient’s strength in their non-brace leg. After the first step, the SBLO adapts in real-time to the user’s walking.

VII. CONCLUSION

The smart bionic leg orthosis (SBLO) developed in this work offers a novel method to alleviate challenges faced by wearers of conventional KAFOs, helping to decrease pain and increase mobility by restoring normal motion characteristics to weak or paralyzed legs. Unlike conventional, fixed knee-ankle-foot orthoses, the SBLO bends the KAFO wearer’s knee during walking. It is easily voice-controlled and automatically adapts to changes in terrain and walking speed. Results from kinetic/kinematic calculations, walking gait testing, and statistical analysis indicate that the objectives of this work were achieved and demonstrate the unique robotic rehabilitation capability provided by the SBLO retrofit. Gen-2 SBLO torque and range of motion resemble that of reference healthy legs, reflecting a significant improvement from conventional fixed

KAFOs. Biomechanical simulations indicate that the force contribution from the SBLO can minimize the additional effort needed by the wearer, reducing excess energy expenditure by more than 30%. Whole-body gait data from a wearable data collection harness confirmed that healthy walking gait was restored across multiple real-life testing conditions; all eight walking gait characteristics evaluated had been normalized across multiple mobility scenarios. Motion in leg segments and joints was normalized by up to 99.84%, and gait pathologies were reduced by up to 78%. The findings suggest that as an inexpensive retrofit to a conventional thermoplastic KAFO, the SBLO offers unique benefits by leveraging biomechatronic capabilities to aid in walking and incorporate rehabilitative assistance throughout daily ambulation. Future work may pursue further improvements to the power efficiency and shock absorption capabilities of the actuation mechanism. In addition, adaptive sensors can be incorporated that are capable of rapidly detecting and reacting to slips and falls [34]. By replicating the efficiency, resilience, and fast reaction times of biological musculature and reflex pathways, such advanced orthoses can offer greater control, comfort, and safety during walking.

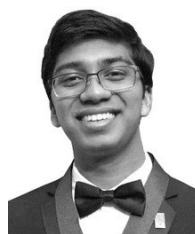
ACKNOWLEDGMENT

The authors would like to thank Dr. Pramatha Payra for reviewing and providing feedback on the industrial process analytics utilized in this study.

REFERENCES

- [1] A. M. Dollar, and H. Herr, “Lower Extremity Exoskeletons and Active Orthoses: Challenges and State-of-the-Art,” *IEEE Trans. Robot.*, vol. 24, no. 1, pp. 144-158, Feb. 2008, DOI: 10.1109/TRO.2008.915453.
- [2] F. Genet, A. Schnitzler, S. Mathieu, K. Autret, L. Theffenne, O. Dizien, A. Maldjian, “Orthotic Devices and Gait in Polio Patients,” *Ann. Phys. Rehabil.*, vol. 53, pp. 51-59, Sep. 2009. DOI: 10.1016/j.rehab.2009.11.005
- [3] J. P. Otto, “The Stance Control Orthosis: Has Its Time Finally Come?” *Orthot. Prosthet. Edge*, Mar. 2008. [Online]. Available: https://opedge.com/Articles/ViewArticle/2008-03_02
- [4] *KAFO (Knee-Ankle-Foot Orthosis)*. Scheck and Sireess, Chicago, IL, USA, Aug. 2016. [Online]. Available: <https://www.scheckandsireess.com/wp-content/uploads/2016/08/KAFO-JM.pdf>
- [5] J. E. Edelstein, and A. Moroz, “Transfemoral Gait Analysis,” in *Lower-Limb Prosthetics and Orthotics: Clinical Concepts*, Thorofare, NJ, USA: SLACK Inc., 2011, ch.10-11, pp. 71-78.
- [6] K. Shamaei, P. C. Napolitano, and A. M. Dollar, “A Quasi-Passive Compliant Stance Control Knee-Ankle-Foot Orthosis”, in *IEEE Int. Conf. Rehabil. Robot. (ICORR)*, Seattle, WA, USA, 2013, pp. 1-6. DOI: 10.1109/ICORR.2013.6650471.
- [7] B. Zacharias, A. Kannenberg, “Clinical Benefits of Stance Control Orthosis Systems: An Analysis of the Scientific Literature,” *J. Prosthet. Orthot.*, vol. 24, no. 1, pp. 2-7, Jan. 2012. DOI: 10.1097/JPO.0b013e3182435db3.
- [8] M. Bellmann, T. Schmalz, S. Blumentritt, “Comparative Biomechanical Analysis of Current Microprocessor Controlled Prosthetic Knee Joints”, *Arch. Phys. Med. Rehabil.*, vol. 91, no. 4, pp. 644-652, 2010. DOI: 10.1016/j.apmr.2009.12.014.
- [9] “C-Brace: World’s First Orthotronic Mobility System” Otto Bock HealthCare GmbH, Duderstadt, DE. [Online]. Available: <https://media.ottobock.com/orthotics/c-brace/files/c-brace-brochure-canada.pdf>
- [10] B. Spencer, “The £60k bionic leg: First Exoskeletal Orthosis goes on sale... it can even help your golf.” *Daily Mail*, Feb. 2015, [Online] Available: <http://www.dailymail.co.uk/news/article-2940175/The-60k->

- [bionic-leg-exoskeletal-orthosis-help-people-minor-disabilities-walk-cycle-play-golf-goes-sale-UK.html](#)
- [11] M. Bortole, A. Venkatakrishnan, F. Zhu, J. C. Moreno, G. E. Francisco, J. L. Pons, and J. L. Contreras-Vidal, "The H2 Robotic Exoskeleton for Gait Rehabilitation after Stroke: Early Findings from a Clinical Study," *J. Neuroeng. Rehabil.*, vol. 12, Jun. 2015. DOI: 10.1186/s12984-015-0048-y.
- [12] C. Hovorka, M. Geil, and M. Lusardi, "Principles Influencing Orthotic and Prosthetic Design: Biomechanics, Device-User Interface, and Related Concepts." in *Orthotics and Prosthetics in Rehabilitation*, 2nd ed., M. Lusardi and C. Nielsen, St. Louis, MO, USA: Saunders Elsevier, 2007, pp. 135-154.
- [13] S. K. Agrawal, S. K. Banala, A. Fattah, V. Sangwan, V. Krishnamoorthy, J. P. Scholz, and W-L. Hsu, "Assessment of Motion of a Swing Leg and Gait Rehabilitation with a Gravity Balancing Exoskeleton," *IEEE Trans. Neural Syst. Rehabilitation Eng.*, vol. 15, no. 3, pp. 410-420, Sept. 2007. DOI: 10.1109/TNSRE.2007.903930.
- [14] C. Mavroidis, R. G. Ranky, M. L. Sivak, B. L. Patriitti, J. DiPisa, A. Caddle, K. Gilhooly, L. Govoni, S. Sivak, M. Lancia, R. Drillio, and P. Bonato, "Patient Specific Ankle-Foot Orthoses Using Rapid Prototyping," *J. Neuroeng. Rehabil.*, vol. 8, no. 1, Jan. 2011. DOI: 10.1186/1743-0003-8-1.
- [15] B. Gilbert and D. Landry, "High Torque Active Mechanism for Orthotic and/or Prosthetic devices," US Patent 8211042B2, Jul. 3, 2012. [Online].
- [16] H. M. Herr and R. D. Kornbluh, "New Horizons for Orthotic and Prosthetic Technology: Artificial Muscle for Ambulation", in *Proc. SPIE vol. 5385, Smart Structures and Materials: Electroactive Polymer Actuators and Devices (EAPAD)*, Jul. 2004. DOI: 10.1117/12.544510.
- [17] R. Williams, "Engineering Biomechanics of Human Motion." Athens, OH, USA: Ohio University, 2016. [Online]. Available: <https://www.ohio.edu/mechanical-faculty/williams/html/PDF/Supplement4670.pdf>
- [18] W. Tao, T. Liu, R. Zheng, and H. Feng, "Gait Analysis Using Wearable Sensors," *Sensors*, vol. 12, pp. 2255-2283, 2012. DOI: 10.3390/s120202255.
- [19] T. Watanabe, H. Saito, E. Koike, and K. Nitta, "A Preliminary Test of Measurement of Joint Angles and Stride Length with Wireless Inertial Sensors for Wearable Gait Evaluation System," *Comput. Intell. Neurosci.*, Sep. 2011. DOI: 10.1155/2011/975193.
- [20] E. Zheng, B. Chen, X. Wang, Y. Huang, and Q. Wang, "On the Design of a Wearable Multi-sensor System for Recognizing Motion Modes and Sit-to-stand Transition," *Int. J. Adv. Robot. Syst.*, vol. 11, no. 30, 2014. DOI: 10.5772/57788.
- [21] T. W. Dorn, J. M. Wang, J. L. Hicks, and S. L. Delp, "Predictive Simulation Generates Human Adaptations during Loaded and Inclined Walking," *PLoS ONE*, vol. 10, no. 4, Apr. 2015. DOI: 10.1371/journal.pone.0121407.
- [22] S. Chowdhury and N. Kumar, "Estimation of Forces and Moments of Lower Limb Joints from Kinematics Data and Inertial Properties of the Body by Using Inverse Dynamics Technique," *J. Rehabil. Robot.*, vol. 1, no. 2, pp. 93-98, 2013. DOI: 10.12970/2308-8354.2013.01.02.3.
- [23] R. Bradford, "Normal Ranges of Joint Motion", in *Stretching and Flexibility*, Bath, Somerset, UK: University of Bath, ch. 8. [Online]. Available: http://people.bath.ac.uk/masrjb/Stretch/stretching_8.html#SEC84
- [24] D. Thompson, "Joint Moments". Univ. of Oklahoma Health Sciences Center, Oklahoma City, OK, USA. Apr. 2001. [Online] Available: <http://ouhsc.edu/bserdac/dthomps/web/gait/epow/jtmom.htm>
- [25] T. Seel, J. Raisch, and T. Schauer, "IMU-Based Joint Angle Measurement for Gait Analysis," *Sensors*, vol. 14, no. 4, pp. 6891-6909, Apr. 2014. DOI: 10.3390/s140406891.
- [26] P. F. Su, S. A. Gard, R. D. Lipschutz, and T. A. Kuiken, "Gait Characteristics of Persons with Bilateral Transtibial Amputations," *J. Rehabil. Res. Dev.*, vol. 44, no. 4, pp. 491-502, Apr. 2007. DOI: 10.1682/JRRD.2006.10.0135.
- [27] A. Rajagopal, C. L. Dembia, M. S. DeMers, D. D. Delp, J. L. Hicks, and S. L. Delp, "Full Body Musculoskeletal Model for Muscle-Driven Simulation of Human Gait," *IEEE Trans. Biomed. Eng.*, vol. 63, no. 10, pp. 2068-2079, Oct. 2016. DOI: 10.1109/TBME.2016.2586891.
- [28] Huei-Ming Chai. "The Gait during Ambulation." Taipei City, Taiwan: National Taiwan University, 2005. [Online].
- [29] J. Doke, J. M. Donelan, and A. D. Duo, "Mechanics and Energetics of Swinging the Human Leg," *J. Exp. Biol.*, vol. 208, pp. 439-445, 2005. DOI: 10.1242/jeb.006767.
- [30] S. L. Delp, F. C. Anderson, A. S. Arnold, P. Loan, A. Habib, C. T. John, E. Guendelman, and D. G. Thelen, "OpenSim: Open-Source Software to Create and Analyze Dynamic Simulations of Movement," *IEEE Trans. Biomed. Eng.*, vol. 54, pp 1940-1950, 2007. DOI: 10.1109/TBME.2007.901024.
- [31] A. Seth, D. Thelen, F. C. Anderson, and S. L. Delp, "OpenSim Musculoskeletal Models." Palo Alto, CA, USA: National Center for Simulation in Rehabilitation Research (NCSRR). [Online]. Available: <https://simtk-confluence.stanford.edu/display/OpenSim/Musculoskeletal+Models>
- [32] B. R. Umberger, "Stance and Swing Phase Costs in Human Walking," *J. R. Soc. Interface*, vol. 7, no. 50, pp. 1329-1340. DOI: 10.1098/rsif.2010.0084.
- [33] R. Kumar, "Process Capability and Process Performance", iSixSigma Reference Guide. Available: <https://www.isixsigma.com/tools-templates/capability-indices-process-capability/>
- [34] S. Payra, G. Loke, Y. Fink, "Enabling Adaptive Robot-Environment Interaction and Context-Aware Artificial Somatosensory Reflexes through Sensor-Embedded Fibers," *IEEE Undergraduate Research Technology Conference (URTC), Oct. 2020. In Press.*



Syamantak Payra (STM'18) is currently a candidate for the SB degree in electrical engineering and computer science at the Massachusetts Institute of Technology (MIT), Cambridge, MA, USA.

He has previously completed internships in a variety of cross-functional industries, including Battery Engineering at Apple, Program Management at Microsoft, and Bioinformatics at the Fondazione Bruno Kessler (Trento, Italy). Passionate about creating technologies with human impact, his research work has included rehabilitation robotics, biomedical sensing, and intelligent fabrics, with further interdisciplinary work across fields like materials science, microbiology, and public policy.

Mr. Payra is an elected member of the Sigma Xi scientific research honor society and has been inducted into the National Gallery for America's Young Inventors. Among his previous research honors are multiple 1st Place Grand Awards at the Intel International Science and Engineering Fair (ISEF), and 9th Place at the 2018 Regeneron Science Talent Search (STS). Recently, he earned the 2nd Place Best Paper Award at the 2020 IEEE Undergraduate Research Technology Conference.



Krishnan Mahadevan received the BE degree in electrical and electronics engineering from Anna University, Chennai, Tamil Nadu, India in 1989, and the MS degree in electrical engineering from Wayne State University, Detroit, MI, USA in 1993.

He has an extensive background in electrical and automotive systems engineering, specializing in real-time embedded systems programming. From 1993 to 2006, he worked as a Systems Engineer at Ford Motor Company, Detroit, MI, and then as a Hardware Engineer at Cummins Incorporated in Charleston, SC. Since 2012, he has been a Faculty with the Department of Information Technology, Green River College, Auburn, Washington, and teaches and consults on cybersecurity and server-client technologies across multiple computing platforms.

Prof. Mahadevan has multiple cybersecurity certifications, including as a Certified Ethical Hacker (CEH), and is an inventor of a patent on automotive powertrain control systems.